

Correlated multiphoton double ionization of helium: The role of nonadiabatic tunneling and singlet recollision

Gennady L. Yudin* and Misha Yu. Ivanov†

Femtosecond Science Program, Steacie Institute for Molecular Sciences, National Research Council of Canada, 100 Sussex Drive, Ottawa, Ontario, Canada K1A 0R6

(Received 17 April 2001; published 15 August 2001)

We study the role of singlet coupling during double ionization of Helium atoms in intense laser fields, within the framework of the recollision model. The singlet cross sections for inelastic $e+\text{He}^+$ scattering, integrated over all excitation and ionization channels, are used. Nonadiabatic corrections during tunneling of the active electron are also included.

DOI: 10.1103/PhysRevA.64.035401

PACS number(s): 32.80.Rm

In our previous publication [1] (see also [2]) we have developed a semiclassical model of intense-field double ionization of noble-gas atoms, based on the physical picture of the recollision between an active electron and its parent ion. Calculations in [1] assumed simple quasistatic tunneling of the active electron and used total inelastic cross sections averaged over the mutual orientation of the electron spins. Here, we discuss the effects of these two approximations by (i) including nonadiabatic corrections to the quasistatic tunneling of the active electron [3] and (ii) using recent theoretical data for singlet $e+\text{He}^+$ cross sections [4–6].

Intense-field ionization in infrared laser fields is often described using the Ammosov-Delone-Krainov formula (ADK) [7]. It is a quasistatic tunneling approximation of the more general expressions derived by Perelomov, Popov, and Terent'ev (PPT) [8] (see also [9]). Quasistatic tunneling approximation is justified in the limit of the Keldysh parameter $\gamma \ll 1$. Here, $\gamma^2 = I_p/2U_p$, I_p is the ionization potential and $U_p = \mathcal{E}^2/4\omega_L^2$ is the average energy of electron oscillations in the laser field, \mathcal{E} is the amplitude, and ω_L is the frequency of the laser field (atomic units are used throughout the paper). However, experimentally one is typically dealing with intermediate values of the Keldysh parameter $\gamma \sim 1$. This is the case in experiments on double ionization of noble gases with $\lambda \approx 800$ nm light.

The PPT expressions give cycle-averaged ionization rates. However, the problem of correlated double ionization requires the knowledge of the subcycle ionization dynamics of the first (active) electron, either for short or for long laser pulses [10]. Simple closed-form analytical expressions for the ionization rate as a function of instantaneous laser phase, for arbitrary values of the Keldysh parameter γ , were obtained in Ref. [3]. These expressions allow us to explicitly distinguish multiphoton and tunneling contributions to the total ionization probability. At $\gamma \sim 1$, the instantaneous laser phase dependence differs dramatically from both the quasistatic tunneling limit of $\gamma \ll 1$ and multiphoton limit of $\gamma \gg 1$. Since subcycle electron dynamics plays a crucial role in the correlated double ionization of Helium, the corrections to quasistatic tunneling should be included.

The result for the instantaneous ionization rate $\Gamma(\theta)$ in a many-cycle pulse, as a function of the instantaneous phase $-\pi/2 \leq \theta \leq \pi/2$ is [3]

$$\Gamma(\theta) = N \exp\left(-\frac{\mathcal{E}^2}{\omega_L^3} \Phi(\gamma, \theta)\right), \quad (1)$$

where the exponential dependence $\Phi(\gamma, \theta)$ is given by the following expression:

$$\Phi(\gamma, \theta) = \left(\gamma^2 + \sin^2 \theta + \frac{1}{2}\right) \ln c - \frac{3\sqrt{b-a}}{2\sqrt{2}} \sin|\theta| - \frac{\sqrt{b+a}}{2\sqrt{2}} \gamma, \quad (2)$$

$$a = 1 + \gamma^2 - \sin^2 \theta,$$

$$b = \sqrt{a^2 + 4\gamma^2 \sin^2 \theta},$$

$$c = \sqrt{\left(\sqrt{\frac{b+a}{2}} + \gamma\right)^2 + \left(\sqrt{\frac{b-a}{2}} + \sin|\theta|\right)^2}.$$

The pre-exponential factor is

$$N = A_{n^*, l^*} B_{l, |m|} \left(\frac{3\kappa}{\gamma^3}\right)^{1/2} C I_p \left(\frac{2(2I_p)^{3/2}}{\mathcal{E}}\right)^{2n^* - |m| - 1}, \quad (3)$$

$$\kappa = \ln(\gamma + \sqrt{\gamma^2 + 1}) - \frac{\gamma}{\sqrt{\gamma^2 + 1}},$$

where the coefficient A_{n^*, l^*} is coming from the radial part of the wavefunction at $r \gg 1/\sqrt{2I_p}$ and depends on the effective principal quantum number $n^* = Z/\sqrt{2I_p}$ (Z is the ion charge) and the effective angular momentum l^* . The coefficient $B_{l, |m|}$ is coming from the angular part of the wave function and depends on the actual angular momentum l and its projection m on the laser polarization vector. The corresponding expressions are [8,9,7]

$$A_{n^*, l^*} = \frac{2^{2n^*}}{n^* \Gamma(n^* + l^* + 1) \Gamma(n^* - l^*)}, \quad (4)$$

*Email address: gennady.yudin@nrc.ca

†Email address: misha.ivanov@nrc.ca

$$B_{l,|m|} = \frac{(2l+1)(l+|m|)!}{2^{|m|}|m|!(l-|m|)!},$$

where $\Gamma(z)$ is the gamma function.

The factor $C = (1 + \gamma^2)^{|m|/2 + 3/4} A_m(\omega_L, \gamma)$ is the Perelomov-Popov-Terent'ev (PPT) correction to the quasi-static limit $\gamma \ll 1$ of the Coulomb pre-exponential factor, with A_m given by Eqs. (55)–(56) of Ref. [8]. The correction C is in practice a slow function of γ . In the limit $\gamma \ll 1$, the factor $C = 1$, while in the limit $\gamma \gg 1$, for $m=0$ one has $A_0 \approx 1.2/\gamma^2$ and $C \approx 1.2/\sqrt{\gamma}$.

Previously [1], we have used spin-averaged cross sections of inelastic e+He⁺ collisions. However, there is an important difference between the usual e+He⁺ collisions and those following tunnel ionization of He: in the latter case, the two electrons involved in the process start in the singlet ground state, and their singlet coupling is preserved during ionization. This effect is virtually absent in other noble gases with many valence electrons.

Calculation of correlated multiphoton double ionization of helium using the approach of Ref. [1] requires the knowledge of the total singlet cross sections σ_{inel}^S of all inelastic channels in e+He⁺ collisions. While there are no experimental data for singlet collisions, there are two recent theoretical calculations. The first used the convergent close-coupling (CCC) approach to obtain total singlet ionization cross sections σ_{ion}^S and partial singlet excitation cross sections σ_{fi}^S for all l, m states of different n shells of He⁺, with $n = 2, 3, 4$, for energies up to 1 KeV [4,5]. The second used the B -spline-based R -matrix approach to obtain total singlet ionization cross sections σ_{ion}^S and partial singlet excitation cross sections σ_{fi}^S for $|1S\rangle \rightarrow |2S, 2P\rangle$ channels for energies up to 175 eV [6].

We note that the absolute values of the ionization cross section in Ref. [6] are clearly less than in [4,5], with deviations ranging from 5% to 50%, depending on the electron energy. On the other hand, $\sigma_{1S \rightarrow n=2}$ is virtually the same in both [4,5] and [6].

Near and below the ionization threshold, the results of [4] exhibit oscillations that we average out following the prescription of [1]. We also note that (i) these oscillations essentially cancel each other in the total inelastic cross section, (ii) in [6] similar oscillations have also been averaged out by the authors.

Here, we are interested in the collision cross sections for electron energies up to $E \sim 400$ eV. We begin with the spin-averaged cross sections. The singlet cross sections are related to the spin-averaged ones via the corresponding asymmetry coefficients, see below.

The spin-averaged cross section for direct ionization σ_{ion}^{Av} [4,11] can be approximated using the general expressions of Ref. [1] based on correct limits at high and near-threshold energies:

$$\sigma_{ion}^{Av}(E) \approx \pi a_0^2 \left(\frac{2 \text{ Ry}}{I_p} \right)^2 F(E/I_p) \quad (5)$$

$$F(x) = \frac{1}{x} \left[A \ln x + B \left(1 - \frac{1}{x} \right) - \frac{C \ln x}{x} \right].$$

Here, a_0 is the Bohr radius, $I_p \approx 54.4$ eV is the ionization potential of He⁺. The data of [4,11] are fit by $B = C = 1$, while $A = 0.285$ is determined from the Bethe-Born limit for the H-like atom [12]. This cross section has a maximum at $E_m \approx 170.6$ eV.

The total excitation cross section includes all channels from $n=2$ to infinity. Using the n^{-3} scaling for high n , it is easy to see that

$$\sigma_{exc} \approx \sigma_{1S \rightarrow n=2} + \sigma_{1S \rightarrow n=3} + 2.45 \sigma_{1S \rightarrow n=4}. \quad (6)$$

We use this expression to obtain the total spin-averaged excitation cross section σ_{exc}^{Av} from the data of Ref. [4]. We find that the scaling introduced in [1] holds, yielding the following semiempirical expression

$$\sigma_{exc}^{Av} \approx \frac{0.101 \pi a_0^2}{1 + 0.31 G(E)}, \quad (7)$$

where $G(E) = (E - I_p)/E_m$.

The singlet cross section is related to the spin-averaged one via the asymmetry coefficient A_{fi} :

$$\sigma_{fi}^S = (1 + 3A_{fi}) \sigma_{fi}^{Av}, \quad (8)$$

where $A_{fi} = (1 - r_{fi})/(1 + 3r_{fi})$ and $r_{fi} = \sigma_{fi}^T/\sigma_{fi}^S$ is the ratio of triplet to singlet cross sections. We note that although the absolute values of the ionization cross sections in Refs. [4,5] and [6] are different, the asymmetry coefficients that one can obtain from these values are virtually identical.

For $|i\rangle = |1S\rangle$ and electron energies $E < 400$ eV we parametrize the asymmetry coefficients as

$$A_{fi} \equiv A_f = \frac{B_f}{1 + C_f G(E) + D_f G^2(E)}. \quad (9)$$

Based on the data of [4,5], we find that the coefficients $\{B_f, C_f, D_f\}$ are $\{0.53, 5.7, 1.0\}$ for $|1S\rangle \rightarrow |n=2\rangle$, $\{0.61, 2.8, 2.0\}$ for $|1S\rangle \rightarrow |n=3\rangle$, and $\{0.66, 2.9, 1.6\}$ for $|1S\rangle \rightarrow |n=4\rangle$. For all excitation channels the coefficients are $\{0.56, 4.0, 1.9\}$, and for the total ionization cross section they are $\{0.63, 0.8, 0.3\}$.

These results, together with Eq. (6), allow us to find the asymmetry coefficient for the total inelastic cross section. For the electron energies $E < 400$ eV, the asymmetry coefficient is

$$A_{inel} = \frac{0.56}{1 + 2.5G(E)}. \quad (10)$$

These results are illustrated in Fig. 1. Figure 1(a) shows A_f for $n=2, 3, 4$ channels and A_{exc} for cross sections summed over all excitation channels. Figure 1(b) compares A_{exc} with A_{ion} and A_{inel} . For all energies except near the threshold $A_{ion} > A_4 > A_3 > A_2$. Since the main contributions to the ex-

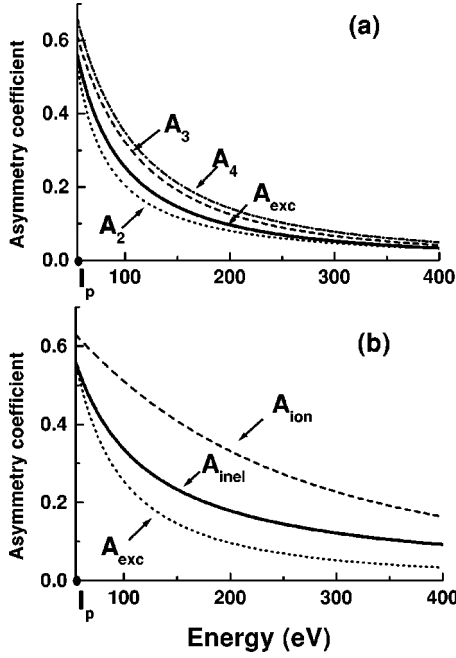


FIG. 1. Asymmetry coefficients for different channels of inelastic $e+\text{He}^+$ collisions, calculated using Eqs. (9),(10) which are based on the data of Refs. [4–6]: (a) excitation to $n=2$ (dot), $n=3$ (dash), $n=4$ (dot-dash), and all excitation channels (solid); (b) all excitation channels (dot), ionization (dash), and all inelastic channels (solid).

citation cross sections σ_{exc}^{Av} and σ_{exc}^S are coming from the $|1S\rangle \rightarrow |n=2\rangle$ channel, A_{exc} is close to A_2 .

With increasing energy, A_{ion} decreases much slower than A_{exc} . This leads to a quantitatively different relationship between ionization and excitation cross sections in the singlet case, compared to the spin-averaged case. While in the latter case, excitation always dominates, in the former case, the singlet cross sections σ_{exc}^S and σ_{ion}^S are very close in the energy range 150–300 eV.

Absolute values of the cross sections based on our expressions and the results of [4,5] are summarized in Fig. 2 for energies above the ionization threshold.

For electron energies below I_p we have used the approximation described in [1], connecting the known value $\sigma_{inel}(I_p)$ with its zero value at the first excitation threshold.

Calculation of the probability of an inelastic collision from the above cross sections is analogous to that described in [1]. Based on the data of [4,5], we take the average excitation energy to be $\bar{\Omega}(I_p) \approx 1.6$ a.u.

Results of our calculations of double ionization of Helium, which follow the prescription of Ref. [1] and use total inelastic cross sections, both singlet and spin-averaged, are shown in Fig. 3 together with the experimental data of Ref. [13]. Figure 3 shows the ratio of the yields of doubly and singly charged ions, $R = N(\text{He}^{2+})/N(\text{He}^+)$, for laser wavelength $\lambda = 780$ nm and intensities $I = 2 \times 10^{14} - 1.4 \times 10^{15}$ W/cm^2 . Compared to [1], we have used expressions for the instantaneous tunneling rate from Ref. [3], see also Eq. (1), thus including the effect of the non-adiabatic tunneling.

We have checked the sensitivity of the results to various

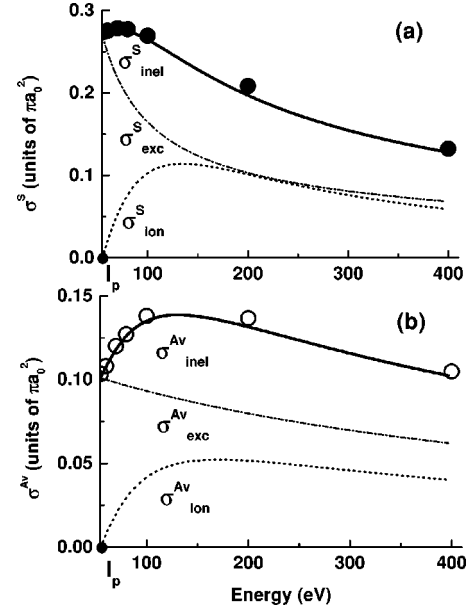


FIG. 2. Cross sections of $e+\text{He}^+$ collisions for excitation, ionization, and all inelastic channels: (a) singlet (dot - ionization, dot-dash - excitation, solid - total), (b) spin-averaged (dot - ionization, dot-dash - excitation, solid - total). The curves are calculated using Eqs. (5),(7),(8),(10). Circles - data based on the results of [4,5].

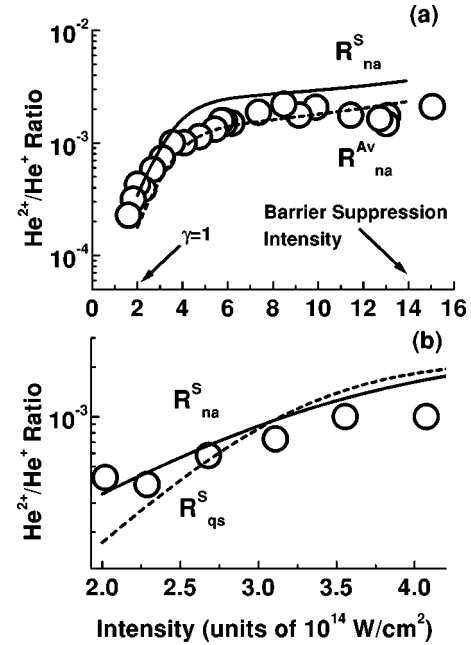


FIG. 3. Ratio of doubly to singly charged He vs laser intensity, for $\lambda = 780$ nm. Circles: experimental data of Ref. [13]. (a) Effect of singlet coupling: dashed and solid curves are calculated using semiclassical recollision model as described in [1], including non-adiabatic tunneling. Dashed curve (R_{na}^{Av}) is obtained using spin-averaged cross sections, solid curve (R_{na}^S) is obtained using singlet cross sections (see text). (b) Effect of nonadiabatic tunneling at $\gamma \sim 1$. Dashed curve (R_{qs}^S) is obtained using quasistatic tunneling model as described in [1], while the solid curve (R_{na}^S) includes nonadiabatic tunneling (see text). Both curves use singlet cross sections.

initial conditions for the position x_0 and the velocity $v_x^{(0)}$ of the active electron along the direction of the electric field, immediately after tunneling. The results differ less than 10% for various ensembles of $x_0, v_{\parallel}^{(0)}$. The results shown in Fig. 3 correspond to x_0 fixed at the point where the electron with the energy $-I_p$ exits the Coulomb barrier, and $v_{\parallel}^{(0)}$ has Gaussian distribution identical to that of $v_{\perp}^{(0)}$ (velocity component perpendicular to electric field),

$$w(v) \propto \exp\left(-\frac{\sqrt{2I_p}v^2}{\mathcal{E}(t)}\right). \quad (11)$$

Both theoretical curves show the same qualitative behavior as experimental data (e.g., display plateau at higher intensities). The effects of nonadiabatic tunneling are most pronounced at lower intensities when $\gamma \sim 1$, see Fig. 3(b).

For our conditions, the effects of singlet coupling can be approximated by a simple empirical formula $R_{na}^S/R_{na}^{Av} \approx 1 + \exp(-I/I_0)$ where $I_0 = 2.2 \times 10^{15}$ W/cm² is determined by

the characteristic energy (proportional to $U_p^{(0)} \propto I_0/\omega_L^2$) at which the singlet effects become small. The ratio is two at low intensities, when the recollision is dominated by the excitation to the $n=2$ shell. In this case, the effect of the singlet coupling is determined by the characteristic ratio of the cross sections $\sigma_{1S \rightarrow n=2}^S/\sigma_{1S \rightarrow n=2}^{Av}$ in the vicinity of I_p .

Quantitatively, the discrepancy between calculations using singlet cross sections and the experimental data is about 30–50% in the plateau region. It is not surprising given the approximate nature of the semiclassical model of double ionization [1]. The discrepancy can also be in part due to the inaccuracy of the cross sections used, which for ionization differ between [4,5,11] and [6].

We acknowledge fruitful discussions with P. Corkum. We are very grateful to I. Bray and D. Fursa for giving us access to the database of electron-ion and electron-atom collision cross sections, to H. van der Hart for stimulating discussions and additional data on singlet cross sections, and to L. DiMauro for providing experimental data of Ref. [13].

-
- [1] G. L. Yudin and M. Yu. Ivanov, Phys. Rev. A **63**, 033404 (2001).
- [2] V. R. Bhardwaj, S. A. Aseyev, M. Mehendale, G. L. Yudin, D. M. Villeneuve, D. M. Rayner, M. Yu. Ivanov, and P. B. Corkum, Phys. Rev. Lett. **86**, 3522 (2001).
- [3] G. L. Yudin and M. Yu. Ivanov, Phys. Rev. A **64**, 013409 (2001).
- [4] I. Bray and Yu. Ralchenko, *Convergent Close-Coupling Data Base*, <http://yin.ph.flinders.edu.au/CCC-WWW/index.html>.
- [5] I. Bray and D. V. Fursa (private communication).
- [6] H. W. van der Hart and K. Burnett, Phys. Rev. A **62**, 013407 (2000); H. W. van der Hart, J. Phys. B **34**, L1 (2001); H. W. van der Hart (private communication).
- [7] M. V. Ammosov, N. B. Delone, and V. P. Krainov, Zh. Éksp. Teor. Fiz. **91**, 2008 (1986) [Sov. Phys. JETP **64**, 1191 (1986)]; N. B. Delone and V. P. Krainov, *Multiphoton Processes in Atoms* (Springer-Verlag, Berlin, 1994).
- [8] A. M. Perelomov, V. S. Popov, and M. V. Terent'ev, Zh. Éksp. Teor. Fiz. **50**, 1393 (1966) [Sov. Phys. JETP **23**, 924 (1966)].
- [9] A. M. Perelomov, V. S. Popov, and M. V. Terent'ev, Zh. Éksp. Teor. Fiz. **51**, 309 (1966) [Sov. Phys. JETP **24**, 207 (1967)]; A. M. Perelomov and V. S. Popov, *ibid.*, **52**, 514 (1967) [*ibid.*, **25**, 336 (1967)]; V. S. Popov, V. P. Kuznetsov, and A. M. Perelomov, *ibid.*, **53**, 331 (1967) [*ibid.* **26**, 222 (1968)].
- [10] P. B. Corkum, Phys. Rev. Lett. **71**, 1994 (1993).
- [11] I. Bray and I. E. McCarthy, J. Wigley, and A. T. Stelbovics, J. Phys. B **26**, L831 (1993).
- [12] H. Bethe, Ann. Phys. (Leipzig) **5**, 325 (1930).
- [13] B. Walker, B. Sheehy, L. F. DiMauro, P. Agostini, K. J. Schafer, and K. C. Kulander, Phys. Rev. Lett. **73**, 1227 (1994).